Description of STS initial instrument concepts (adapted from First Experiments Spallation Neutron Source Second Target Station)

8.7 STS Instrument Concepts

The full complement of 22 beamlines at the STS will support a suite of neutron scattering instruments that provide wholly new capabilities to the US research community. As part of the STS project, an initial suite of eight instruments will be built; for each instrument, this includes (1) the infrastructure to transport the neutrons from the moderators to the sample position and to shape, manipulate, and shield the neutron beam as required along the incident flight path; (2) the instrument end station and its associated shielding, mechanical components, neutron detectors, and an initial suite of sample environment equipment; and (3) the data management infrastructure and scientific software required to reduce and analyze data.

The research community will be engaged in an instrument selection process early in the preliminary design phase of the STS project to select the initial suite of instruments. A 2015 user community workshop [Eskildsen and Khaykovich, 2015] reviewed a number of proposed STS instrument concepts. Figure 8.6 shows 16 of these notional instrument concepts, distributed around the STS target monolith. Eight of these instruments were identified as high priorities for detailed concept development to support preparation of the STS Conceptual Design Report, and brief descriptions of these instrument concepts are presented in this section. These instruments are subject to refinement, additions, or changes based on future community input. Instrument performances have been calculated with detailed Monte Carlo simulations and show gains of up to three orders of magnitude compared to existing instruments, with the potential to deliver extraordinary new capabilities for the scientific user community.

8.7.1 SANS Instrument

Small-angle neutron scattering (SANS) will benefit from combining the high brightness of STS with next-generation detector technology to probe real-time nanoscale changes in materials that are inaccessible today. This will provide new opportunities to study time-resolved phenomena and kinetics associated with materials processing, 3D printing, or the assembly of complex polymers or biological

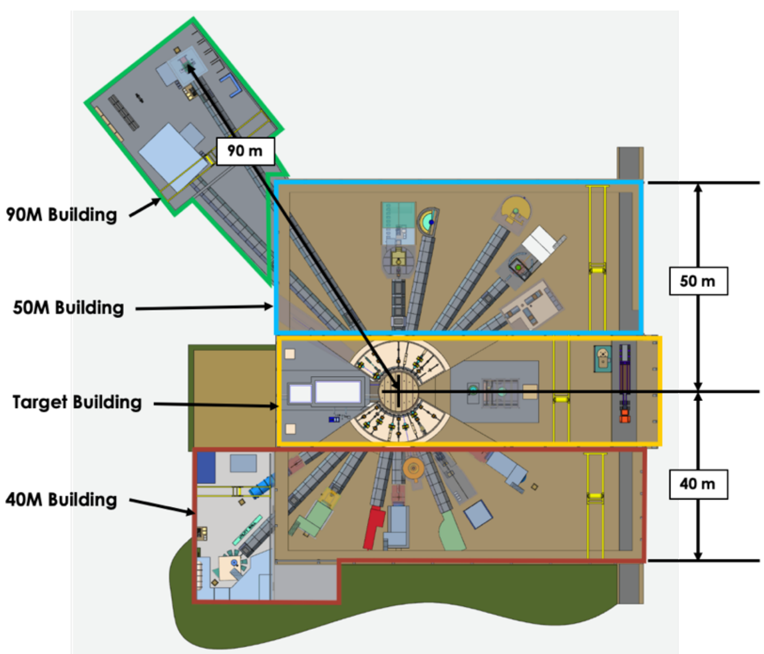

Fig. 8.6. Schematic view of the STS target building and experiment halls, showing 16 of the 22 instruments that will be part of the STS when it is fully outfitted. For clarity, some beamlines have been left unoccupied. Image source: ORNL.

complexes, domain wall and topological defect dynamics in magnets and ferroelectrics, and synthesis of nanomaterials and quantum materials.

For example, SANS at the STS will provide insight into the substructures of cell membranes and as a tool for revealing the structure of membrane-less organelles associated with diseases such as amyotrophic lateral sclerosis without inducing damage to the sample during time-resolved studies. This proposed instrument will be used to characterize the structure of materials from 0.4 nm to hundreds of nanometers across a very broad range of science.

Building on recent success at SNS with advances in neutron chopper technology, the proposed instrument will incorporate a high-speed statistical chopper that enables discrimination of elastic (desired signal) from inelastic (background) scattering, improving the signal-to-noise ratio and resolving a long-standing complication in the operation of TOF SANS instruments. The instrument will use stepped arrays of 30 × 30 cm^2 silicon photomultiplier (SiPM) Anger camera detector modules to support the high anticipated data rates of the instrument, as illustrated in Fig. 8.7. The three detector arrays coupled with the broad wavelength band at the STS mean that the instrument can collect data simultaneously across a broad dynamic range of momentum transfers (Q_{max}/Q_{min}) of about 300–800, depending on the selection of wavelength band. Figure 8.8 shows a Monte Carlo simulation demonstrating the resolution of the instrument using a pseudo-sample that produces a sequence of sharp peaks that are logarithmically spaced in momentum transfer [Lefmann and Nielsen, 1999]. Key instrument parameters are listed in Table 8.1.

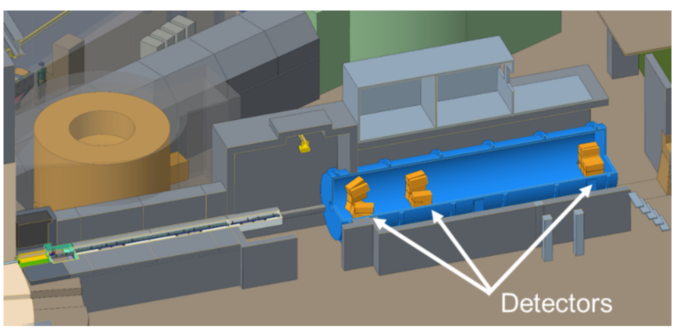

Fig. 8.7. Arrangement of stepped arrays of Anger camera detector modules for the STS SANS instrument. Image source: ORNL.

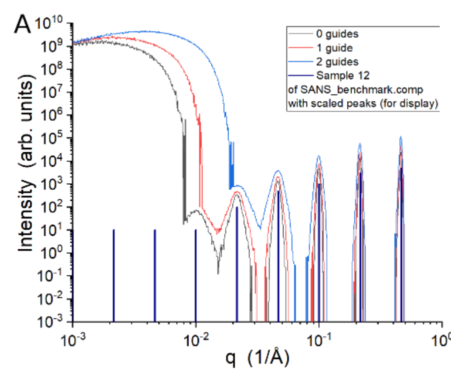

Fig. 8.8. Simulated scattering patterns for the STS SANS instrument. The very sharp diffraction peaks demonstrate the resolution of the instrument. Image source: ORNL.

Table 8.1. STS SANS instrument concept: Key parameters

Parameter	Description
Moderator	Horizontal tube moderator
Beam size	30 × 30 mm^2 guide dimension, nominal 1 cm diameter sample size
Moderator-sample distance	25.2 m (nominal)
Sample-detector distance	1.111 m, 3.333 m, 10.0 m
Detector	Arrays of 30 × 30 cm^2 SiPM Anger camera detectors with 3 × 3 mm^2 pixels for mid-and high-angle banks, as low as 1 × 1 mm^2 pixels for low-Q bank
Q-range (high collimation setting)	0.0017 Å^{-1} < Q < 1.4668 Å^{-1} at 2.0 Å < λ < 9.49 Å (15 Hz) 0.0009 Å^{-1} < Q < 0.2933 Å^{-1} at 10.0 Å < λ < 17.49 Å (15 Hz) 0.0009 Å^{-1} < Q < 1.4668 Å^{-1} at 2.0 Å < λ < 16.98 Å (7.5 Hz)

8.7.2 Simultaneous SANS/WANS Instrument

Simultaneous SANS/wide-angle neutron scattering (WANS) will bridge the gap in length scales between those measured on conventional diffractometers and SANS instruments to simultaneously study the evolution of structure from the subangstrom scale to ≈300 nm. The instrument exploits the wide bandwidth of the STS to provide continuous coverage across this range of length scales, at which interactions govern the properties and function of many complex hierarchical materials, such as high-entropy alloys and polymers. This approach of combining SANS with wide-angle diffraction capabilities has been implemented on the TAIKAN instrument at the Japan Proton Accelerator Research Complex (J-PARC) [Takata et al., 2010], but the wide bandwidth at the STS will make such an instrument feasible for the first time at a US neutron source.

The neutron scattering capabilities of this SANS/WANS combination will be further enhanced with additional in situ characterization tools, such as spectroscopic measurements, to build a more complete, time-resolved picture of sample response to changing environmental conditions. The instrument will simultaneously measure structures across a dynamic range (Q_{max}/Q_{min}) approaching four orders of magnitude. The high brightness of the STS will enable time-resolved measurements of materials in action or as they are being processed. These capabilities will have an immediate impact on the understanding of soft matter systems under real-world processing conditions, for example. Early studies that can be anticipated include real-time spatially resolved measurements of polymer mixtures in millifluidic sample environments, elucidating the mechanism of self-assembly, and crystallization of polymers induced by single-wall carbon nanotubes. The large dynamic range will be particularly effective for measuring systems exhibiting hierarchical structures and crystallization from complex solutions, which can occur in flowing complex fluids such as those used in fracking and various industrial processes.

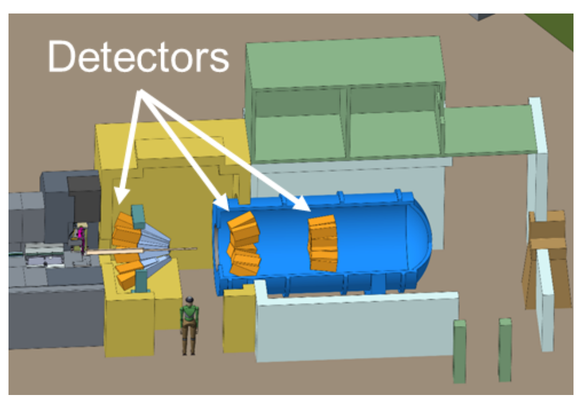

Fig. 8.9. Detector configuration for STS SANS/WANS instrument concept. Image source: ORNL.

Three arrays of 30 × 30 cm^2 SiPM Anger camera detector modules will be used to support the high data rates of this instrument (see Fig. 8.9). The detector locations have been chosen to support a flat sample geometry consistent with low-angle SANS and backscattering diffraction. The detector arrangement provides continuous coverage in momentum transfer at 15 Hz when configured for a minimum wavelength of less than 2 Å. Continuous coverage is maintained to a minimum incident wavelength of 4 Å when the instrument is operated at 7.5 Hz in frame-skipping mode. As with the SANS instrument concept, inclusion of a correlation chopper is under consideration. Table 8.2 lists key parameters for this proposed instrument.

Table 8.2. STS SANS/WANS instrument concept: Key parameters

Parameter	Description
Moderator	Vertical cylinder moderator
Beam size	20×20 mm^2 guide dimension, nominal 1 cm diameter sample size
Moderator-sample distance	30.25 m (nominal)
Sample-detector distance	–1.25 m (backscattering), 1 m (mid-angle), 3 m (low-angle)
Detector	Arrays of 30×30 cm^2 SiPM Anger camera detectors with 3×3 mm^2 pixels
Q-range	0.00373 Å^{-1} < Q < 24.918 Å^{-1} at 0.5 Å < λ < 8.4 Å (15 Hz)
	0.00316 Å^{-1} < Q < 6.229 Å^{-1} at 2.0 Å < λ < 9.9 Å (15 Hz)
	0.00158 Å^{-1} < Q < 3.115 Å^{-1} at 4.0 Å < λ < 19. 8 Å (7.5 Hz)

8.7.3 Neutron Reflectometer with Horizontal Sample Surface

A neutron reflectometer with a horizontal sample surface will enable real-time studies of interfaces including free liquids and the transport of atoms, molecules, or charge across interfaces. Many advanced properties sought through materials by design will only be realized in new materials having at least one nanoscale dimension where new functionality can arise from surface-dominated forces and interactions. New insights unlocked by this instrument will be key to enabling the creation of next-generation batteries, environmentally responsive coatings, drug delivery systems, and sensors.

Early experiments will utilize this brightness to investigate previously inaccessible regimes of real-time structural change on surfaces and interfaces. These experiments will be particularly relevant to new technologies for energy storage devices—for example, reaction pathways for the structural evolution of polyelectrolytes on surfaces or various interfaces in batteries, including solid-solid or solid-liquid. This instrument will enable real-time studies of surface corrosion under various in situ conditions and will have enough intensity to permit detailed studies of heterogeneous mixtures of lipids and other molecules that form biological membranes.

The increased bandwidth of the STS instrument makes it possible to collect complete specular reflectivity curves using a single instrument setting, enabling cinematic operation with continuous observation of the sample as it evolves in time or in response to external stimuli. Samples in time-dependent environments (e.g., temperature, electrochemical, magnetic, or chemical alteration) will be observed in real time, as fast as 1 Hz in favorable cases, such as that shown in Fig. 8.10, which illustrates the ability of the STS reflectometer concept to measure the kinetics of the crosslinking reaction of a polyelectrolyte hydrogel. The engineering concept for this instrument is shown in Fig. 8.11.

To measure reflectivity from samples that must be held horizontal, such as a liquid surface, the neutron beam must be inclined at a small angle, up to approximately 2.5°, relative to the horizontal. Some samples, such as free liquid interfaces where there is a gaseous atmosphere above the liquid, require the neutron beam to reach the interface from above. In this case, the neutron beam is inclined downward from the horizontal. In other cases, such as some liquid-liquid interfaces or when using specialized sample environments such as a rheometer, the neutron beam must reach the interface from below. In this case the neutron beam is inclined upward from the horizontal. This beam line provides both neutron beam geometries with a lower station using a downward-directed beam and an upper station using an upward-directed beam. The two end stations can operate independently and simultaneously support two independent experiments at the same time, each using a different neutron beam geometry, as indicated in Fig. 8.11. Table 8.3 lists the key parameters of this instrument.

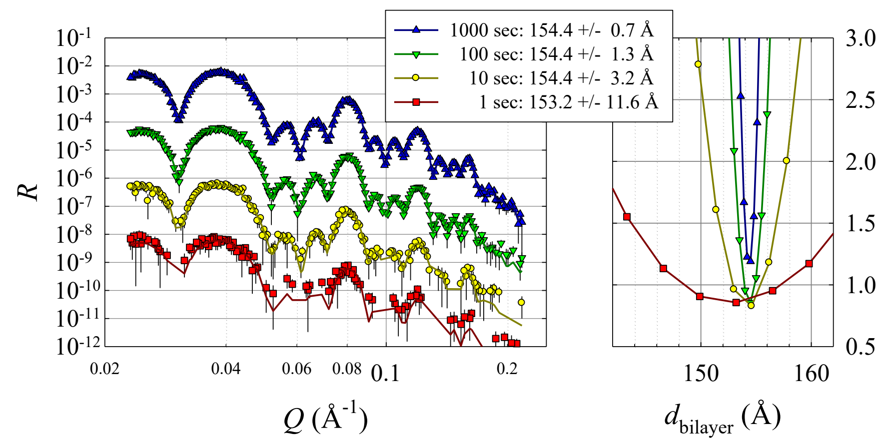

Fig. 8.10. Kinetics of the crosslinking reaction of a polyelectrolyte hydrogel. Left: Simulated 7.5 Hz reflectivity data from a polyelectrolyte multilayer for several collection times at a single incident beam angle of 2.5º. Right: dependence of χ_2 for the fitted value of the marker-layer spacing. Image source: ORNL.

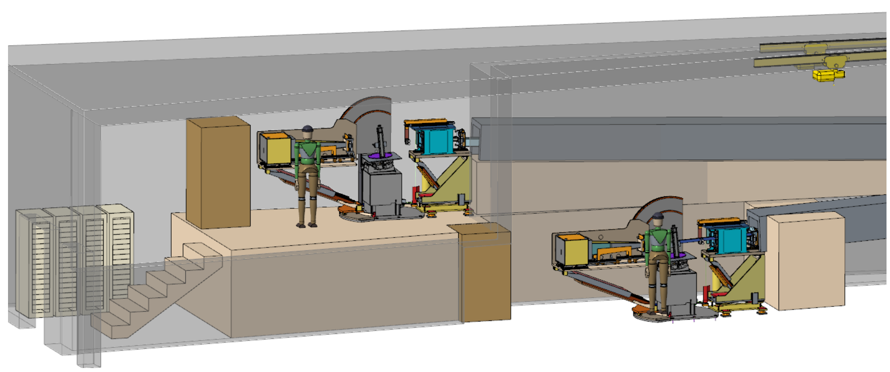

Fig. 8.11. Schematic view of the STS horizontal surface reflectometer concept. The two end stations enable the neutron beam to reflect from below the sample surface (upper) and from above the sample surface (lower). Image source: ORNL.

Table 8.3. STS horizontal surface reflectometer concept: Key parameters

Parameter	**Description**
Moderator	Vertical cylinder moderator
Beam size	20 × 30 mm^2, delivered by a horizontally curved, vertically tapered guide
Moderator-sample distance	20 m (lower end station)
Sample-detector distance	1.5 m (nominal)
Detector	SiPM pixelated scintillator detector, 40 × 20 cm^2, with 2 × 2 mm^2 pixels (inclined detector gives effective 1 × 2 mm^2 pixels)
Q-range	0.009 $Å^{-1} < Q < 0.088$ $Å^{-1}$ at 1.0° incident angle
	0.023 $Å^{-1} < Q < 0.219$ $Å^{-1}$ at 2.5° incident angle
	0.037 $Å^{-1} < Q < 0.351$ $Å^{-1}$ at 4.0° incident angle

8.7.4 Cold Neutron Chopper Spectrometer

A direct geometry inelastic spectrometer can be designed to probe the weak signals intrinsic to small cross sections (e.g., small magnetic moments) or the limited sample sizes often available for new materials or associated with extreme sample environments, such as high pressure. This instrument will be optimized for the study of quantum and functional materials, but its broad dynamic range is also well matched to measuring diffusion and excitations in soft and biological matter. It will have the ability to simultaneously measure dynamic processes over a wide energy range, as indicated in Table 8.4, making it the spectrometer of choice for first measurements of new materials. This instrument will support a polarized neutron beam and polarization analysis to separate nuclear from magnetic scattering and coherent from incoherent scattering processes in hydrogenous materials.

Table 8.4. STS cold neutron chopper spectrometer optimized for small sample area: Key parameters

Parameter	Description
Moderator	Horizontal tube moderator
Beam size	10×10 mm^2
Moderator-sample distance	29.5 m
Sample-detector distance	2.5 m
Detector	25 mm diameter linear position-sensitive detector (PSD), ^{3}He
E_i range	0.5 meV < E_i < 25 meV; with repetition rate multiplication, the source pulse will be subdivided to 5–10 incident energies across a bandwidth of 7–8 Å
ħω resolution	Flexible, $\Delta\hbar\omega$ =2–5% E_i at the elastic line

This instrument will have an immediate impact on research in quantum materials, revolutionizing the energy-momentum resolved spectroscopy in highly entangled systems such as quantum spin liquids. The huge intensity will enable pump-probe experiments to investigate out-of-equilibrium quantum dynamics in many systems, one prototypical example being the behavior of magnetic monopoles in "spin ice" following a pulse of terahertz radiation. The high brightness and large bandwidth of the STS will be utilized for novel investigations of dynamics in quantum materials under extreme pressure, expanding our understanding of phenomena such as topological transformations or emergent collective ground states such as pressure-induced superconductivity. This instrument will be equally useful for understanding new functional materials that can only be synthesized at high pressures. The high brightness will allow investigations of excitations in small-volume systems, including artificial heterostructures and small single crystals.

This instrument will use repetition rate multiplication methods to utilize multiple incident neutron energies sequentially within a single 15 Hz pulse of the STS, making it well suited to perform survey and discovery experiments. Figure 8.12 illustrates this mode of operation with the primary source pulse at 15 Hz subdivided into six incident neutron energies. This ability to simultaneously measure dynamic processes over a wide energy range makes this spectrometer uniquely valuable for surveying materials with excitations covering a large dynamic range where different values of incident energy are needed to provide full coverage at appropriate resolutions. This method is implemented on spectrometers at J-PARC [Nakamura et al., 2009] and has been proposed on a similar instrument concept developed for the ESS [Vickery and Deen, 2014]. In Fig. 8.13, the performance of the STS and FTS chopper spectrometers is compared, illustrating the power of repetition rate multiplication to effectively survey reciprocal space and zoom in on smaller regions with higher resolution when needed [Sala, 2018]. The key parameters of this instrument are listed in Table 8.4.

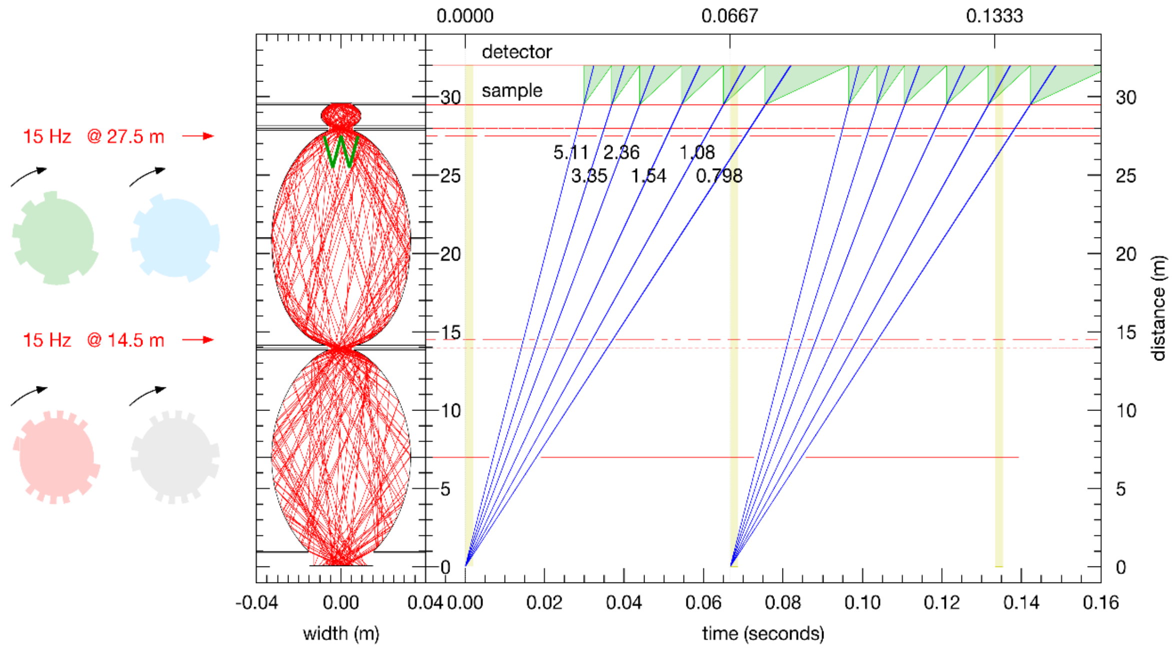

Fig. 8.12. Functional layout of the STS cold neutron chopper spectrometer concept. The time-distance diagram at right illustrates the neutron paths through the guide system (red) and the location of critical components to sort mini-pulses arising from repetition rate multiplication. The incident energies available in a single source pulse are shown for one configuration of the instrument. Image source: ORNL.

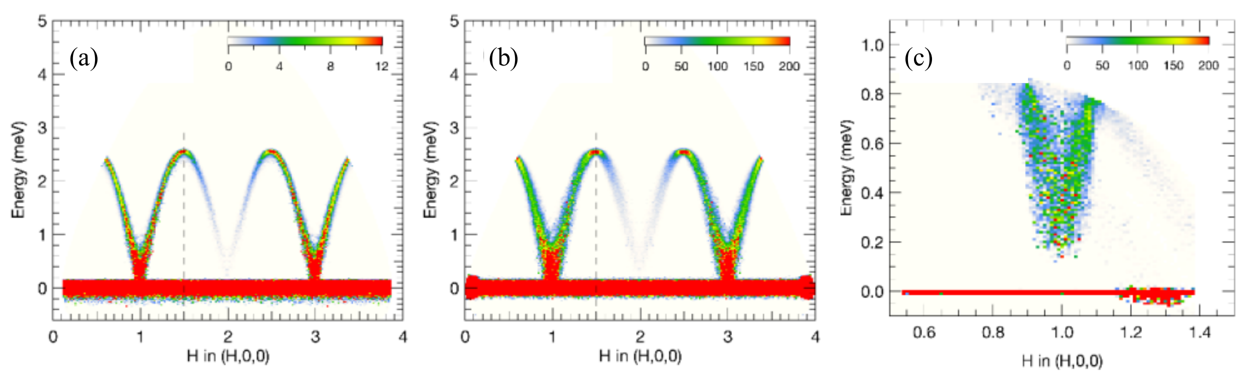

Fig. 8.13. Performance of the FTS and STS cold neutron chopper spectrometers. Spectra calculated for a 1 g sample of $K_2V_3O_8$ for (a) the FTS chopper spectrometer and (b) the STS cold neutron chopper spectrometer at incident neutron energy of 5.1 meV. The intensity is indicated by the color scale at the top of the figures. (c) Benefit of repetition rate multiplication using the 1.08 meV incident energy simultaneously available within a single source pulse to provide higher energy resolution. Image source: ORNL.

8.7.5 Multimodal Instrument for Studies at High Magnetic Field

A multimodal instrument for studies at high magnetic field is designed to collect both indirect geometry spectroscopy and single-crystal diffraction data. This instrument will offer unmatched opportunities to elucidate the structure and dynamics of quantum materials at extremes of magnetic field and low temperatures. A dedicated magnet installation is required to achieve the highest steady-state magnetic fields, similar to the approach taken for the EXED instrument at the Helmholtz Zentrum Berlin BER II reactor [Smeibidl et al., 2010]. Recent advances in composite conductors using high-temperature superconductors provide a pathway to fields as high as 35 T or beyond in a vertical geometry that is best suited for neutron scattering [Hahn et al., 2019]. The high-brightness, focused cold neutron beams of the STS are ideally matched to illuminate the small sample area intrinsic to achieving the highest magnetic field. This multimodal instrument will open new frontiers in the study of quantum critical phenomena, entangled quantum states, and competing magnetic interactions.

Inelastic neutron scattering under extreme magnetic fields provides detailed quantitative access to the spin Hamiltonian of frustrated magnetic materials by measuring the magnon spectrum in the fully polarized high-field state. The Hamiltonian embodies all relevant information needed to develop a theory of lower field collective properties. The proposed instrument, with its extreme high magnetic field, will greatly expand the materials to which this technique can be successfully applied by crossing new thresholds in the minimum field required to saturate the magnetization. The capacity for unprecedented exploration of both structure and dynamics in phases appearing as a result of field-induced quantum critical points will enable progress on a variety of problems; a classic example is the pseudogap phase hidden beneath the dome in unconventional cuprate superconductors.

Extreme high magnetic fields impose severe limitations on the neutron scattered beam geometry, greatly restricting the vertical and horizontal angular ranges that can be accessed. The proposed instrument will use the broad range of wavelengths available in a single pulse to make the best use of the limited detector view of the sample afforded by an ultrahigh-field magnet. The concept for this instrument has eight arms spaced around the magnet in the horizontal scattering plane, providing access to the sample for incident, transmitted, and scattered neutron beams, as illustrated in Fig. 8.14. These arms will be equipped either with diffraction detectors or with a set of sequential crystal analyzers to enable spectroscopy. The multiple analyzer crystals in each spectroscopy arm, combined with the broad range of incident neutron energies within each STS source pulse, enable the instrument to sweep broad ranges of Q-ω space simultaneously [Groitl et al., 2016]. Figure 8.15 illustrates the range of energy and momentum transfers that can be simultaneously accessed by the inelastic arms using both the (002) and (004) reflections of pyrolytic graphite analyzers at 15 Hz when the instrument is configured to use incident neutron wavelengths of 1 to 5 Å. Table 8.5 lists the key parameters of this instrument.

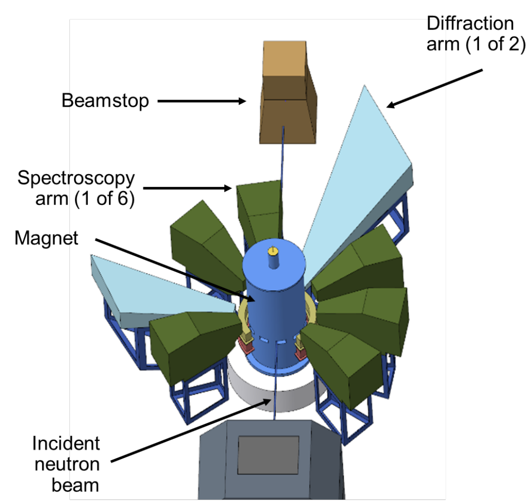

Fig. 8.14. Spectrometer and diffraction arms surrounding the magnet of the multimodal instrument concept. Image source: ORNL.

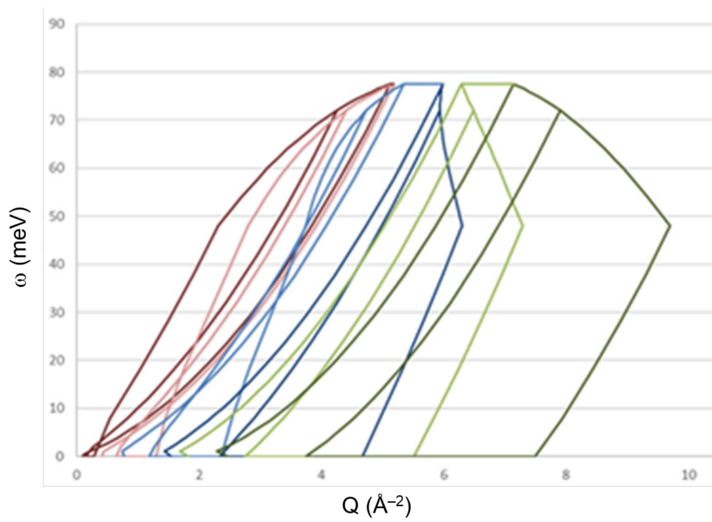

Fig. 8.15. Range of energy and momentum transfer simultaneously accessed by the analyzer arms of the multimodal instrument concept for a single instrument configuration. Image source: ORNL.

Table 8.5. STS multimodal high magnetic field instrument: Key parameters

Parameter	Description
Moderator	Vertical cylinder moderator
Beam size	15×15 mm^2
Moderator-sample distance	55 m
Sample-detector distance	3.5 m to diffraction detectors, varied for analyzer arms
Detector	8 mm diameter linear PSD, ^{3}He
E_i range	3.3 meV < E_i < 80 meV (15 Hz operation, low λ range)
ħω resolution	Δħω =3–8% E_i at the elastic line
Q-range (diffraction arms)	0.4 Å^{-1} < Q < 8.9 Å^{-1} (15 Hz operation, high λ range)

8.7.6 Single-Crystal Diffractometer for Small Samples

A single-crystal diffractometer for small samples will be optimized for collecting Bragg diffraction data from crystal volumes below 0.01 mm^3 with unit cell edges between 10 and 300 Å. The broad wavelength range available in a single STS pulse coupled with the high detector angular coverage of this instrument will enable complete data sets to be collected rapidly, in some cases with only a single orientation of the single-crystal sample. This diffractometer will cross a new threshold in minimum sample crystal sizes, bringing the hydrogen sensitivity of neutrons to new systems, with implications for developing improved drugs to fight multi-drug-resistant viruses and bacteria, understanding enzyme mechanisms, and exploiting the regulation of metabolic pathways for synthetic biology, such as capturing solar energy by mimicking plant photosynthesis. Early experiments will include a crystallographic investigation of PLP-dependent enzymes that should explain how these proteins catalyze so many disparate biological enzyme reactions. The high brightness will also enable detailed crystallographic characterization of the photosynthesis process in the membrane protein known as photosystem II, which proceeds via a specific set of intermediate states.

This proposed instrument features a sophisticated optics system designed for precise control over the neutron phase space delivered to the sample position, as illustrated in Fig. 8.16 [Coates and Robertson, 2017]. The primary slit defining the view of the STS moderator is demagnified by a factor of 30 to produce a beam size at the sample of 1 to 0.001 mm^2. Initial calculations demonstrate that this optics system delivers about twice as many desired neutrons to the sample area as a conventional elliptical guide and about 1000× fewer undesired neutrons to the vicinity of the sample. Monte Carlo simulation shows a very homogeneous neutron distribution at the sample position with flux of 7.64×10^6 n/s/mm^2 integrated over the 15 Hz operating wavelength band from 1.5 to 4.5 Å. Table 8.6 lists key parameters of the instrument.

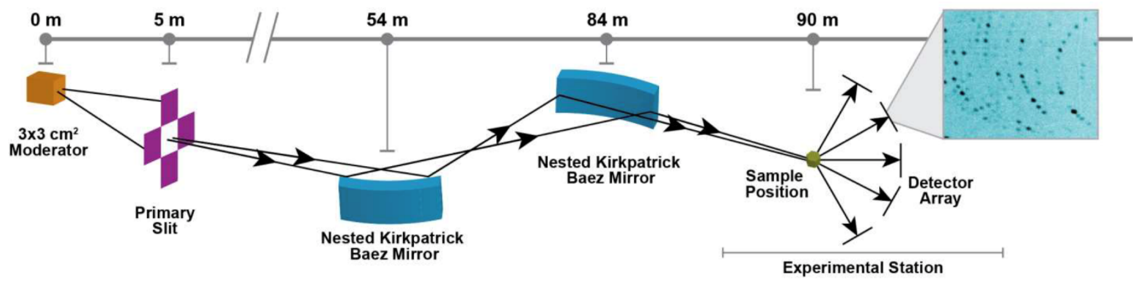

Fig. 8.16. Schematic of the optics design for STS single-crystal diffractometer for small samples. Image source: Coates and Robertson [2017].

Table 8.6. STS single crystal diffractometer for small samples: Key parameters

Parameter	Description
Moderator	Vertical cylinder moderator
Beam size	Variable from 1–0.001 mm^2; controlled by primary slit
Moderator-sample distance	90 m
Sample-detector distance	0.3 m
Detector	(37–116) × 116 mm^2 SiPM Anger cameras with 0.3 × 0.3 mm^2 pixels
d-spacing range	d_{min} = 0.6 Å

8.7.7 Versatile Diffractometer for Magnetic Structure Studies

A versatile diffractometer for magnetic structure studies at the STS will be world-leading for diffraction studies of magnetism in powders and single crystals, allowing routine measurements of milligram-size samples, small magnetic moment compounds, and diffuse signals. This instrument will probe magnetic local and long-range ordering in quantum materials that exhibit emergent properties arising from collective behavior. These experiments are expected to reveal fundamental behavior in quantum magnets that will help drive development and understanding of the next generation of quantum materials, which have the potential to transform computers and data storage and raise the efficiency of energy storage and transmission.

This diffractometer will be equipped with full polarization capability and will be optimized for studies under extreme conditions of temperature, pressure, and magnetic field. Its unique use of polarized neutrons to isolate the magnetic signature in the measured data will enable detailed insight into local magnetic ordering. Planned early applications include polarized diffraction studies of complex topological structures, such as those in noncollinear magnetic systems exhibiting topological spin structures, including skyrmions. The instrument will also enable previously unfeasible measurements of the full crystal structure of the high-pressure metal hydride superconductors, including hydrogen positions.

This proposed instrument uses a mirror optics system to flexibly deliver either high resolution (low beam divergence) or high flux and includes an option to polarize the incident neutron beam. The instrument will use a curved supermirror analyzer to provide full polarization capability. The detector layout will be a logarithmic spiral, similar to that employed on the POWGEN diffractometer at the FTS, to preserve the required resolution at low *Q* by increasing the distance from the sample to the low-angle detectors, as illustrated in Fig. 8.17.

At present, the Wish instrument at ISIS Target Station 2 (ISIS-TS2) is widely considered the world-leading powder diffractometer for magnetic studies. The operating frequencies of ISIS-TS2 (10 Hz) and the STS (15 Hz) are similar; however, the peak brightness at the STS will be more than an order of magnitude larger, and the instrument will receive 50% more pulses than Wish. Table 8.7 lists key parameters of the instrument.

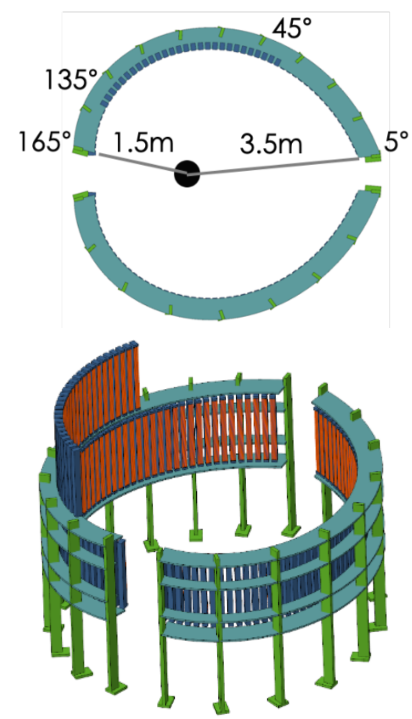

Fig. 8.17. Detector layout for STS diffractometer optimized for magnetic structure studies. Top: View of detector array from above. Bottom: 3D view of detector array. The distance from sample to detector has been selected to preserve the resolution at low *Q* required for magnetic studies. Image source: ORNL.

Table 8.7. STS diffractometer optimized for magnetic structure studies: Key parameters

Parameter	Description
Moderator	Vertical cylinder moderator
Beam size	Variable from 3 × 3 mm^2 (single crystal) to 10 × 20 mm^2 (powders); controlled by primary slit
Moderator-sample distance	40 m
Sample-detector distance	1.5 m to 3.5 m (detectors arranged in logarithmic spiral)
Detector	^{3}He linear PSDs (1 m long, 10 mm in diameter), 1792 tubes
Q-range	$0.1\ \text{Å}^{-1} < Q < 12.5\ \text{Å}^{-1}$ at $1\ \text{Å} < \lambda < 6.75\ \text{Å}$ (15 Hz, first frame operation)
Q resolution	$\Delta Q/Q \approx 0.3\%$

8.7.8 Versatile Multiscale Materials Engineering Beamline

A versatile multiscale materials engineering beamline at the STS will be a transformational high-flux instrument with unique capabilities for the study of low-symmetry, complex materials. It will support both fundamental and applied materials science and engineering research in a broad range of fields, including advanced alloy design, energy storage and conversion, nuclear energy, aerospace, transportation, and civil infrastructure. This instrument will combine unprecedented long-wavelength neutron flux and high detector coverage to enable real-time studies of complex structural and functional materials behavior under mechanical, thermal, electrical and magnetic fields. It will incorporate SANS and imaging capabilities to extend its sensitivity to larger length scales and higher spatial resolution. First experiments are expected to include studies of model alloys exhibiting phase transitions proceeding via metastable states as a function of temperature and strain, with simultaneous measurements of both atomic (i.e., crystal) and microstructural features, as well as texture. Another initial application will be to characterize the real-time structural changes occurring during processing of materials, for example during additive manufacturing.

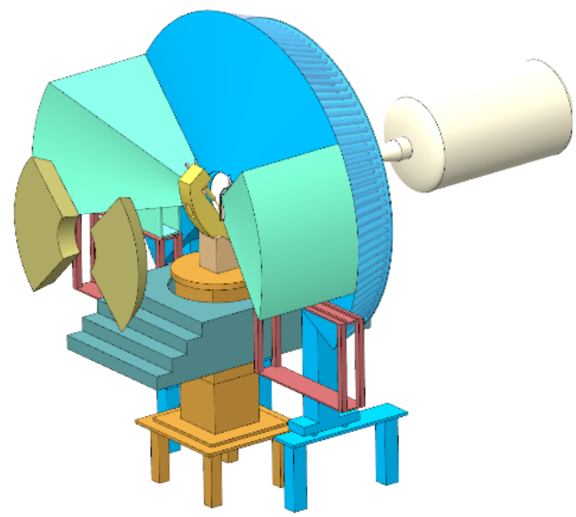

Fig. 8.18. Detector layout for the STS engineering materials instrument. At right, ~5 m from the sample, is a SANS detector. Two detector banks positioned at ~90° are shown in light green, while detector banks that are particularly useful for measuring orientational data are shown in blue. The remaining detector bank, shown in dark tan, provides high-resolution backscattering measurements. Image source: ORNL.

As is the case for the other two STS diffractometer concepts, this proposed instrument will use a mirror optics system to flexibly deliver the desired neutron phase space to the sample location. The unique detector geometry illustrated in Fig. 8.18 provides the capability to measure noncoplanar components of strain and complete orientation distributions for textured samples with a minimum number of simple sample rotations about a single axis. Figure 8.19 compares the performance of this instrument with the FTS engineering diffractometer VULCAN for measurement of diffraction peaks in a Ni_3Al superalloy with a superlattice structure (note the change in vertical axis scale). The optimized cold neutron moderator at the STS, coupled with advanced neutron optics, will deliver a cold neutron flux to the sample up to three orders of magnitude higher than VULCAN at wavelengths greater than about 5 Å. VULCAN views a thermal moderator and was optimized for thermal neutron performance using neutron wavelengths from about 0.5 Å to 3 Å. In contrast, the STS instrument has been optimized to use neutron wavelengths from 2 Å to 10 Å Figure 8.19 shows the additional weighting given to long *d*-spacings by the cold spectrum relative to the thermal spectrum of VULCAN. The STS instrument will complement the strengths of VULCAN, which uses the

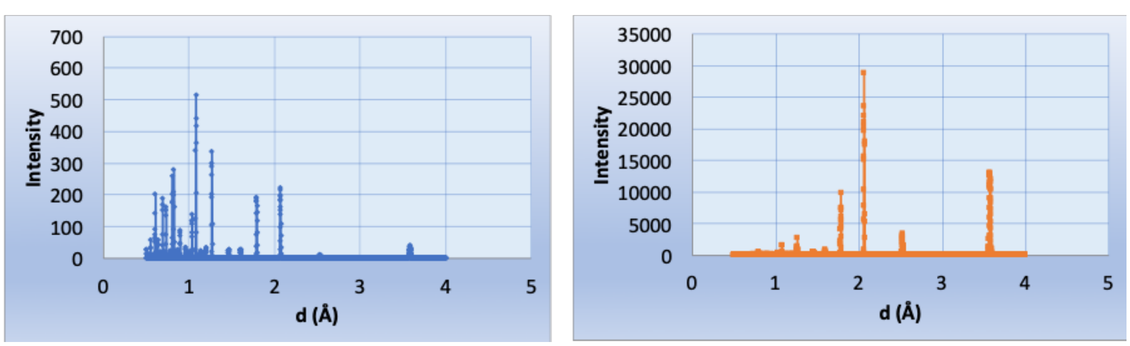

Fig. 8.19. Simulated diffraction data from VULCAN at the FTS (left) and the engineering diffractometer at the STS. Identical gauge volumes and counting time was used in the simulations. Note difference in vertical axis scale. Image source: ORNL.

high-wavelength resolution of thermal neutrons available on the FTS to study high-symmetry crystal structures. Table 8.8 lists key parameters of the proposed instrument.

Table 8.8. STS multiscale engineering beamline: Key parameters

Parameter	Description
Moderator	Vertical cylinder moderator
Beam size	1–10 mm^2 in high-intensity mode; up to 1 cm^2 in high-resolution mode
Moderator-sample distance	72 m
Sample-detector distance	Variable depending on detector bank; up to 5 m for SANS
Detector	^{3}He linear PSDs (0.7 m and 1 m long, 8 mm in diameter); B/Gd-doped microchannel coupled to Timepix readout
d-spacing range	0.5 Å < d_{min} < 7.9 Å in 7.5 Hz frame-skipping mode

References for Sect. 8

Coates, L.; Robertson, L. *J. Appl. Crystallogr.* **2017,** *50,* 1174–1178.

Eskildsen, M. R..; Khaykovich, B. (co-chairs). *Second Target Station Workshop Report,* UT-Battelle, LLC, Oak Ridge, TN, 2015. Available at https://neutrons.ornl.gov/sites/default/files/STS Workshop Report.pdf (accessed June 13, 2019).

Groitl, F.; Graf, D.; Birk, J. O.; Markó, M.; Bartkowiak, M.; Filges, U.; Niedermayer, C.; Rüegg, C.; Rønnow, H. M. *Rev. Sci. Instrum.* **2016,** *87,* 035109.

Hahn, S.; Kim, K.; Kim, K.; Hu, X.; Painter, T.; Dixon, I.; Kim, S.; Bhattari, K. R.; Noguchi, S.; Jaroszynski, J.; Larbalestier, D. C. *Nature* **2019,** *570,* 496–499.

Lefmann, K.; Nielsen, K. *Neutron News* **1999,** *10,* 20.

Nakamura, M.; Kajimoto, R.; Inamura, Y.; Mizuno, F.; Fujita, M.; Yokoo, T.; Arai, M. *J. Phys. Soc. Japan* **2009,** *78,* 093002.

Sala, G.; Lin, J. Y. Y.; Graves, V. B.; Ehlers, G. *J. Appl. Crystallogr.* **2018,** *51,* 282–293.

Smeibidl, P.; Tennant, A. D.; Ehmler, H.; Bird, M. *J. Low Temp. Phys.* **2010,** *159,* 402–405.

Takata, S.; Suzuki, J.; Shinohara, T.; Oku, T.; Tominaga, T.; Ohishi, K.; Iwase, H.; Nakatani, T; Inamura, Y.; Ito, T.; Suzuya, K.; Aizawa, K.; Arai, M.; Otomo, T; Sugiyama, M. *JPS Conf. Proc.* **2010,** *8,* 036020.

Vickery A.; Deen, P. P. *Rev. Sci. Instrum.* **2014,** *85,* 115103.